Catal Lett (2009) 128:363–372
DOI 10.1007/s10562-008-9755-3

Benzoylation of Anisole over Silicotungstic Acid Modified Mesoporous Alumina

S. Selvakumar · A. P. Singh

Received: 15 September 2008 / Accepted: 23 October 2008 / Published online: 11 November 2008

Abstract Mesoporous alumina (MA) molecular sieves were synthesized by using aluminum sec-butoxide as Al precursor and lauric acid as the structure directing agent. The synthesized MA was functionalized with silicotungstic acid (STA) via wet impregnation method and characterized by various physico-chemical techniques. The XRD patterns of a series of HPA functionalized MA are showing the ordered structures. N_2 sorption analysis shows type IV isotherm. NH_3–TPD measurements revealed an increase in number of acid sites with an increase in loading of STA over MA. At the same time decrease in the acidity was observed with the increase in calcination temperature of the supported materials. Functionalization of STA were also carried out over different alumina supports such as catapol-B (CB) and alumina synthesized without surfactant (ASW) and their activities were evaluated by carrying out liquid phase Friedel–Craft acylation (FC) reaction of anisole with *p*-toluoyl chloride in a batch reactor at 120 °C. Recycling was performed in the FC reaction using 30 wt% STA–MA two times and no major deactivation of the catalyst was observed.

Keywords Mesoporous alumina · Silicotungstic acid · Friedel–Craft acylation

1 Introduction

Synthesis of highly acidic inorganic materials by heterogenization of homogeneous systems is currently the subject of a great deal of research in green chemistry that aims to facilitate the recovery of the catalyst and to minimize the pollution. Many acidic catalysts have been developed using silica, titania, metal oxides, and microporous zeolites as supports [1–5]. However, there are still many problems because of limited acidity and diffusion. After the successful synthesis of mesoporous silica by Mobil researchers, [6, 7] many attempts have been made to prepare mesoporous non siliceous materials by using the concept of the surfactant-templating route. Niobium, hafnium, and cerium based materials are now frequently cited [8–10]. However, as noted in a review by Sayari and Liu [11], although a large number of elements are able to form such materials, only few of these exhibits ordered porous structures. Among the different non siliceous mesoporous materials porous alumina is attractive with broad applicability as adsorbents, catalyst supports, and as part of bifunctional catalysts in large-scale processes in the chemical and petrochemical industry. However, its non uniform pore size, low porosity, and low surface area limit its potential application for catalyzing reactions. The possibility of obtaining such material with a mesoporous texture has made this oxide even more interesting. Due to the importance of alumina in catalysis, the ability to tailor its pore system is needed, and thus, several attempts have been made to synthesize mesoporous aluminas. Various surfactants have been used as template to direct the formation of mesostructures via interactions between the organic templates and the inorganic precursors, e.g. via hydrogen bonding or electronic interactions. Pinnavaia et al. were the first to report the preparation of mesostructured wormhole-like alumina from aluminum tri-sec-butoxide in the presence of electrically neutral, block-copolymer surfactants as structure-directing agents [12, 13]. Similar wormhole structures have also been

S. Selvakumar · A. P. Singh (✉)
Inorganic and Catalysis Division, National Chemical Laboratory, Pune 411008, India
e-mail: ap.singh@ncl.res.in

synthesized by the hydrolysis of aluminum alkoxides assisted by the anionic surfactant sodium dodecylbenzenesulfonate [14] or the cationic surfactant cetyltrimethylammonium bromide [15].

Friedel–Crafts acylation and benzylation of aromatic compounds is an important transformation in organic synthesis leading to aromatic ketones. Traditionally, these reactions are carried out by using homogeneous catalysts such as $AlCl_3$, BF_3, $TiCl_4$, $SnCl_4$ or strong protic acids (such as HF and H_2SO_4). However, the commonly used homogeneous Lewis acid catalysts pose several problems, such as difficulty in separation and recovery from the reaction products, use in more than a stoichiometric amount of a Lewis acid is needed in many cases due to coordination of the Lewis acids to aromatic ketones produced. The workup commonly requires hydrolysis of the complex, leading to the loss of the catalyst and giving large amounts of corrosive waste streams.

Heteropoly acids (HPAs) are Bronsted acids composed of heteropoly anions and protons as countercations. HPAs are stronger than many conventional solid acids such as mixed oxides and zeolites. HPAs catalyze a wide variety of reactions in homogeneous phase offering strong option for efficient and cleaner processing. It has been recognized that a major drawback of HPA is its low thermal stability when applied to high-temperature reactions, low surface area (1–10 m^2/g) and separation problem from reaction mixture [16]. Although the thermal stability depends on the structure and composition of HPAs, the total decomposition of Keggin structure generally occurs at temperatures up to 723–823 K to give the mixed oxides composed of HPAs [17]. HPAs can be made ecofriendly insoluble solid acid with high thermal stability and high surface area by supporting them onto suitable supports. The support provides an opportunity to HPAs to be dispersed over a large surface area, which increases catalytic activity. Major factors contributing to the catalytic activity are nature of support, loading and conditions of pretreatment. Various supports like silica, [18–22] titania [23, 24] active carbon [25–28] MCM-41 [29–31], acidic ion exchange resins [32] have been used for supporting HPAs. Hence, we thought that the immobilization of HPAs over mesoporous alumina would develop a novel class of heterogeneous solid acid catalysts with enhanced acidity. Moreover, the use of a heterogeneous HPAs system would offer ease of catalyst recovery and reuse, and minimize the production of waste currently formed during recovery.

In this paper, we disclose the preparation of silicotungstic acid (STA) functionalized mesoporous alumina using mesoporous alumina as solid support and STA as an acidic component. The nature of support and support-STA interaction was determined by different techniques. The activity of the catalyst was examined by Friedel–Craft (FC) acylation reaction of anisole with *p*-toluoyl chloride (*p*-TC) to 4-methyl-4′-methoxy benzophenone (4,4′-MMBP).

2 Experimental

2.1 Materials

Aluminium tri-sec-butoxide, lauric acid, and 1-propanol were procured from across organics, Aldrich and Merck, respectively. Silicotungstic acid ($H_4SiW_{12}O_{40} \cdot xH_2O$) was purchased from Loba chemie limited. Catapol-B is a boehmite form of Al_2O_3 was purchased from Condea-German chemical company, having the surface area 240 $m^2\ g^{-1}$. All the chemicals were research grade and used as received without further purification.

2.2 Preparation of Mesoporous Alumina (MA)

Mesoporous alumina was prepared from the gel with the following composition, aluminium tri-sec-butoxide/lauric acid/1-propanol/H_2O 1:0.3:30:3.1 [14]. Typically, an aluminium hydroxide suspension was prepared by the hydrolysis of 54.8 g of aluminium tri-sec-butoxide with 12.4 g of deionised water in 400 g of 1-propanol (99%). After stirring for 1 h, 13.6 g of lauric acid (99.5%) was added slowly to the gel mixture. The mixture was aged for 24 h at room temperature and then heated under static conditions at 110 °C in a round bottomed flask for 2 days. The solid material obtained was then filtered, washed with ethanol and dried at 100 °C for 4–5 h. Finally, the material was calcined at 550 °C with a temperature ramp of 1 °C/min from room temperature to the final temperature.

The catalysts were prepared by wet impregnation method using mesoporous alumina as the support. To a methanolic solution of silicotungstic acid, mesoporous alumina powder was added and the mixture was stirred for 8–10 h. The excess of methanol was evaporated to dryness and the obtained product was dried at 120 °C and calcined in air at 250 °C [33]. A series of catalysts with different STA loading (5–40%) on mesoporous alumina was prepared and calcined at 250 °C. In order to study the influence of calcination temperature on the catalytic activity, catalyst with 30 wt% STA loading on mesoporous alumina was calcined at three different temperatures (250, 450 and 650 °C).

2.3 Characterization

Synthesized catalysts were characterized by X-ray diffraction using a Rigaku Miniflex powder diffractometer on finely powdered samples using Cu Kα radiation and 30 kV and 15 mA. The XRD patterns were recorded for 2θ

between 0.5 and 5 then 10–80, at a scan rate of 2°/min. Adsorption of nitrogen was carried out at 77 K using a NOVA 1200 (Quanta chrome) apparatus for analyzing surface areas and pore-size distributions of the synthesized catalysts. Specific surface areas were calculated following the BET procedure. Pore-size distribution was obtained by using the BJH pore analysis applied to the desorption branch of the nitrogen adsorption/desorption isotherms. FT-IR spectra of solid samples were taken in the range of 4000–400 cm^{-1}on a Shimadzu FT-IR 8201 instrument. Thermo gravimetric analyses (TGA and DTA) were performed using a Diamond TG/DTA instrument, from 30 to 1000 °C at a heating rate of 10 °C/min under airflow. NMR spectra were recorded on a DPX200 Bruker spectrometer. Experiments on the saturation adsorption of ammonia and its subsequent temperature-programmed desorption (TPD–NH_3) were performed on a Micromeritics Autochem 2910 instrument. About 0.1 g of a fresh sample was placed in a U-shaped, flow-through, quartz micro reactor for each experiment. The catalyst was activated at 220 °C for 2 h under He flow (30 mL/min) and then cooled to 100 °C before being exposed to ammonia. The sample was flushed again in He for 1 h to remove any physisorbed ammonia, and a desorption profile was then recorded by increasing the sample temperature from 100 to 900 °C at a ramp rate of 10 °C/min.

2.4 Friedel–Craft Acylation Reaction of Anisole with *p*-toluoyl Chloride

Anisole and *p*-toluoyl chloride were used without further purification. The catalyst was activated at 100 °C for 2 h before use in the experiments, so as to maintain the dry conditions. The FC reaction was performed in a 50 mL round bottom flask fitted with a condenser. The temperature of the reaction vessel was maintained using an oil bath. In a typical run, a mixture of anisole (5 mmol), *p*-toluoyl chloride (5 mmol) and activated catalyst (0.1 gm), was magnetically stirred and heated to attain the reaction temperature (120 °C). The product samples were withdrawn at regular intervals of time and analyzed periodically on a gas chromatograph (Agilent 6890 N) equipped with a flame ionization detector and a capillary column (5 μm thick cross-linked methyl silicone gum, 0.2 mm × 50 m long). The main product, 4-methyl-4′-methoxy benzophenone is separated by column chromatography and confirmed by ^{1}H and ^{13}C NMR analysis. ^{13}C NMR ($CDCl_3$, 50 MHz) δ 21.5 (–CH_3), 55.36 (–OCH_3), 195.27 (–CO–), 135.36 (1), 130.31 (2, 6), 128.77 (3, 5), 142.52 (4), 129.89(1′), 132.32 (2′, 6′), 113.37 (3′, 5′), 162.92 (4′). ^{1}H NMR ($CDCl_3$, 200 MHz) δ 2.43 (S, 3H), 3.87 (S, 3H), 6.95 (D, J = 8.84 Hz, 2H), 7.26 (D, J = 7.83 Hz, 2H), 7.67 (D, J = 8.21 Hz, 2H), 7.81 (D, J = 8.85 Hz, 2H).

3 Results and Discussion

3.1 X-ray Diffraction (XRD)

The powder X-ray diffraction (XRD) patterns of all the synthesized catalysts are shown in Fig. 1. The small angle X-ray diffraction patterns of calcined and STA modified samples show an intense single peak at high ‘d’ spacing typically observed for mesoporous materials featuring

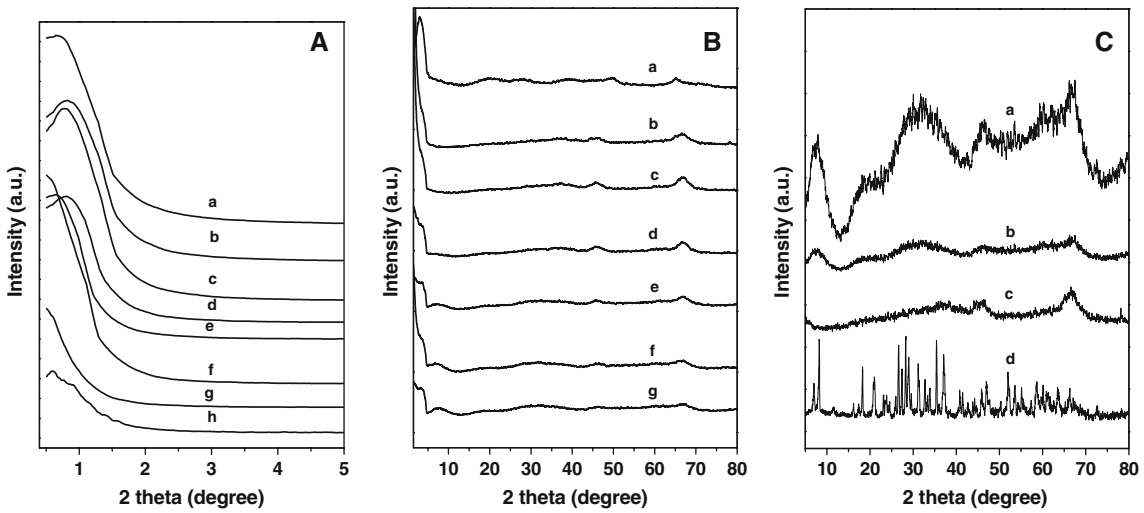

Fig. 1 XRD pattern of **A** (a) calcined MA (b) 5 wt% STA–MA (c) 10 wt% STA–MA (d) 20 wt% STA–MA (e) 30 wt% STA–MA (f) 30 wt% STA–ASW (g) 50 wt% STA–MA (h) 30 wt% STA–CB. **B** (a) As-synthesized-MA (b) calcined MA (c) 5 wt% STA–MA (d) 10 wt% STA–MA (e) 20 wt% STA–MA (f) 30 wt% STA–MA (g) 30 wt% STA–WSA **C** (a) 50 wt% STA–MA (b) 30 wt% STA–MA (c) calcined MA (d) pure STA

randomly order pores [34] whereas STA loaded catapol-B and alumina synthesized without surfactant didn't show such peak. An increase in the intensity of the XRD line is observed upon removal of the surfactant from the MA (Fig. 1A). This may be because of the electron density between the inorganic walls and the pores become progressively larger as the organic is decomposed [14]. Figure 1A shows that the mesoporous structure remained intact up to 30 wt% STA loading and further loading looses its mesoporosity subsequently. Figure 1B, C show the wide angle XRD pattern of the as-synthesized and calcined mesoporous alumina along with STA loaded MA. The high angle reflection of mesoporous alumina is showing the γ-phase [35] and STA modified materials start showing bulk STA peaks above 30 wt% loading. This indicates that 30 wt% loading of STA on MA is optimum and STA is well dispersed uniformly inside the pores of mesoporous channels.

3.2 Nitrogen Sorption Studies

The textural property of plain, modified mesoporous alumina, catapol-B and alumina synthesized without surfactant are shown in Table 1. All the isotherms show type IV behaviour demonstrated for mesoporous materials. The surface area, pore volume and pore diameter of the calcined MA is found to be 295 $m^2\ g^{-1}$, 0.56 $cm^3\ g^{-1}$ and 50 Å, respectively, which decreased to 214 $m^2\ g^{-1}$, 0.25 $cm^3\ g^{-1}$ and 41.76 Å, respectively, after 30 wt% STA loading on MA. The decrease in pore volume and pore diameter of the STA modified MA shows the proper impregnation of the materials inside the MA. The pore volume and surface area of the 30 wt% STA loaded commercial alumina (catapol-B) is lower than that of the 30 wt% STA loaded MA. The pore size distribution (PSD) curve of alumina synthesized without surfactant (ASW) and catapol-B (CB) (Fig. 2A) are very broad and indicates that these materials are having a very broad range of mesopores.

3.3 FT-IR Spectra

The as-synthesized, calcined and supported mesoporous alumina with STA were analyzed by FTIR in order to confirm the presence of the Keggin anion on Al_2O_3 mesophase. Figure 3A shows the FTIR spectra of as-synthesized, calcined and STA modified aluminas. All the samples show a strong and broad band in the region of 3600–3200 cm^{-1} corresponding to the hydrogen bonded–OH group. Similarly a broad band centered at 1640 cm^{-1} is seen in all samples corresponding to the bending mode of the adsorbed water molecule. The as-synthesized material shows band in the region of 2800–2900 cm^{-1} corresponding to the –C–H stretching frequency of the surfactant. The Al–O–Al bending modes (symmetric and asymmetric) are observed at 1077 and 1165 cm^{-1}, respectively [36]. Figure 3B shows the FTIR spectra of (a) 30 wt% STA loaded MA (b) calcined MA (c) 20 wt% STA loaded MA in the region between 400 and 1600 cm^{-1}, finger print region of the metal oxygen bonds. The metal

Table. 1 Summary of the catalyst property

Sample	BET surface area ($m^2\ g^{-1}$)	Pore diameter (Å)	Pore volume ($cm^3\ g^{-1}$)
Calcined MA	295	50.00	0.56
30 wt% STA–MA	214	41.76	0.25
30 wt% STA–ASW	230	Broad	0.32
30 wt% STA–CB	110	Broad	0.22

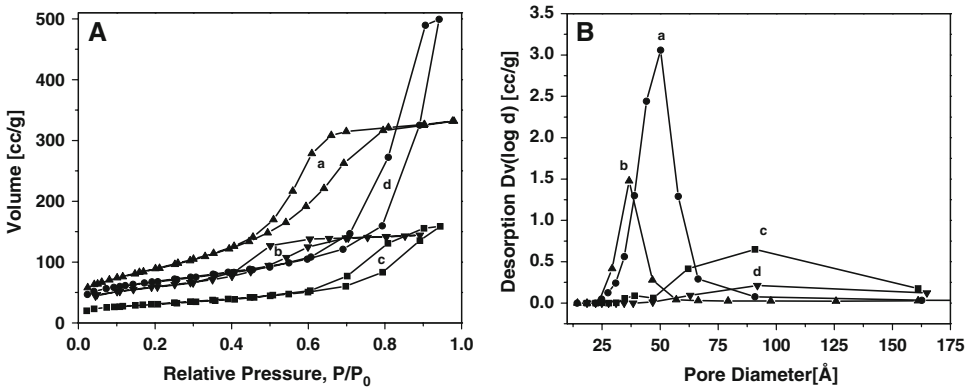

Fig. 2 N_2 adsorption–desorption isotherms and pore-size distribution of (**A**, **B**) (a) calcined MA (b) 30 wt% STA–MA (c) 30 wt% STA–CB (d) 30 wt% STA–ASW

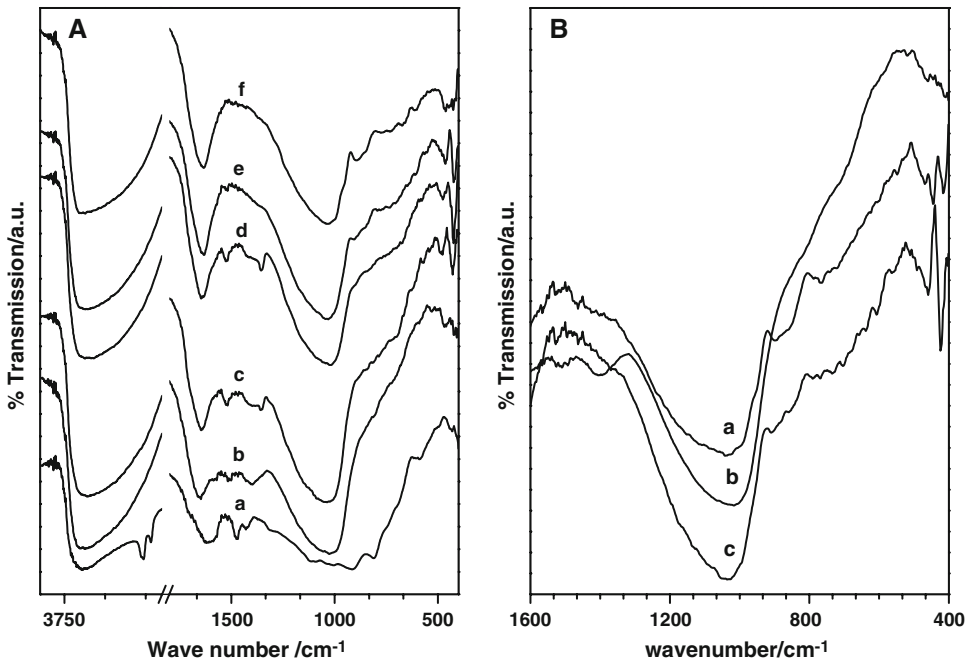

Fig. 3 FT-IR spectrum of **A** (a) as-synthesized-MA (b) calcined MA (c) 5 wt% STA–MA (d) 10 wt% STA–MA (e) 20 wt% STA–MA (f) 30 wt% STA–MA. **B** (a) 30 wt% STA–MA (b) calcined MA (c) 20 wt% STA–MA

oxygen bands for pure STA ($W = O_t$, W–O_c–W and W–O_e–W) normally appear at 983, 898 and 797 cm^{-1}, respectively, which are not seen after heterogenization of STA on MA due to the broadness of MA band in this region.

3.4 Thermal Analysis

Figure 4 represents the TGA (inset) and DTG pattern of as-synthesized MA, calcined MA, pure STA and 30% STA loaded MA, respectively. The TGA curve of as-synthesized MA is showing two weight losses. The first weight loss below 150 °C corresponds to the removal of physisorbed water molecule. The significant second weight loss that occurred in the region 200–500 °C is attributed to the removal of the surfactant molecule. The TG–DTG analysis of pure STA shows three stages of weight loss. The first weight loss around 2.8% occurred between room temperature and 100 °C corresponds to physisorbed water. The second one around 3.1%, in the range of 100–250 °C, accounted for the loss of crystallization water and the third weight loss ~0.9%, in the range of 250–500 °C, was due to the loss of water molecule originating from all acidic protons [37]. Calcined mesoporous alumina shows only one weight loss below 150 °C corresponds to the removal of physisorbed water molecule. The TGA behavior was similar in the case of 30 wt% STA supported MA compared to calcined materials which shows weight loss corresponds to physisorbed water molecule. The supported sample didn't show any appreciable change in weight loss.

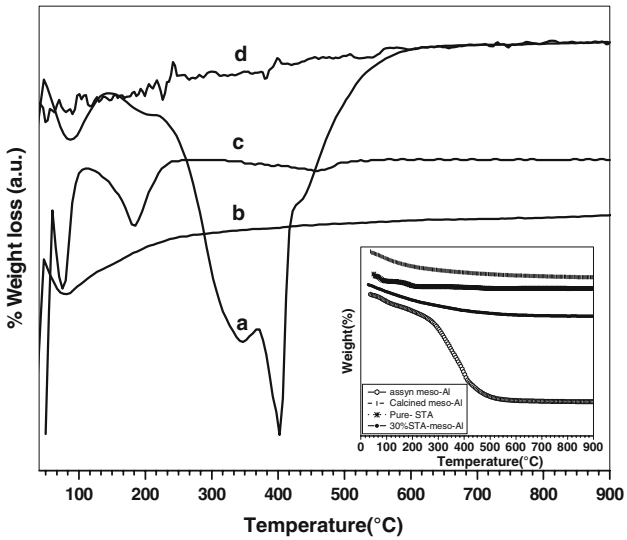

Fig. 4 DTG pattern of (a) As-synthesized-MA (b) calcined MA (c) pure STA (d) 30 wt% STA–MA (inset = TGA pattern)

3.5 ^{27}Al CP/MAS NMR Spectra

MAS NMR is an indispensable tool in characterization of the coordination of aluminum in mesoporous aluminas. The ^{27}Al MAS NMR spectra of the calcined mesoporous alumina and 30% STA loaded mesoporous alumina are depicted in Fig. 5. The calcined sample is showing two distinct aluminium sites at 3.8 and 61.8 ppm [14] indicating octahedral and tetrahedral coordination, respectively. The similar peaks are observed in the case of STA loaded material also with minor shift.

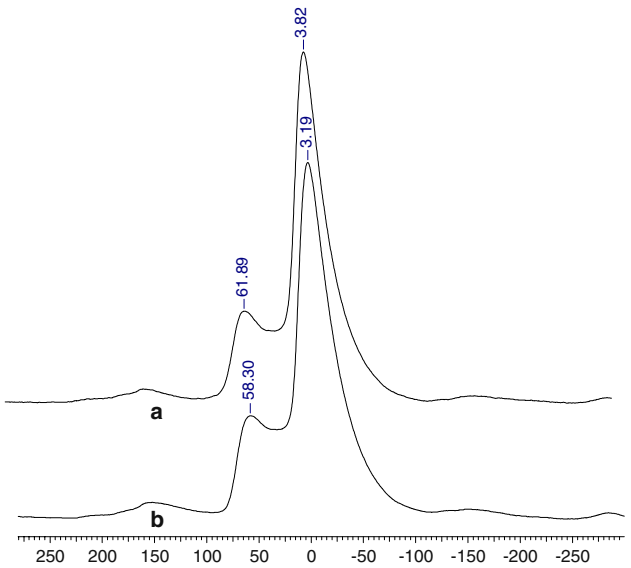

Fig. 5 ^{27}Al CP/MAS NMR spectra of (a) calcined MA (b) 30 wt% STA–MA

3.6 Acidity Measurement

The process of ammonia adsorption–desorption on catalysts is widely applied for the determination of surface acidity. The amount of ammonia adsorbed at high temperature is usually taken as a measure of acidity. Ammonia was used as adsorbate because all acid sites on the catalyst surface are accessible for NH_3 molecules, and the molecules are more selectively adsorbed in the presence of sites of different strengths. Acidity measurement was performed for various STA loaded catalysts. In a typical run, 0.1 g of the catalyst sample was dehydrated at 250 °C for 2 h under He flow (30 mL/min) and then cooled down to 100 °C before being exposed to ammonia. The sample was flushed again for 6 h by He to desorb any physisorbed ammonia. A desorption profile was then recorded by increasing the catalyst temperature from 100 to 900 °C at a ramp rate of 10 °C/min in the flow of 30 mL/min helium.

The total number of acid sites on the catalysts was found to increase proportionally with increased loading of STA over MA (Fig. 6C). At the same time the total acidity value of 30 wt% STA loaded on ASW is more than the similar amount of STA loaded on MA (Fig. 6A, B). It is also evident from these data that high acidity was observed with sample heated at 250 °C and further the acidity get decreased when the calcination temperature of the material increased beyond 250 °C. This may be due to decomposition of the Keggin structure of the heteropoly acid when the calcination temperature increased. This is evidenced by TGA spectra of the pure heteropoly acid (Fig. 4C).

3.7 Catalytic Activity of Various Catalysts

The results of the catalytic activities in the Friedel–Crafts (FC) reaction of anisole with *p*-toluoyl chloride using pure MA support, pure STA, $AlCl_3$, Al–MCM-41, W–meso-Al, STA loaded catapol-B (STA–CB), STA loaded alumina without surfactant (STA–ASW) and STA loaded mesoporous alumina (STA–MA) are depicted in Table 2. The activities of various catalysts are compared under identical reaction conditions using data after 6 h run. The main product of the reaction is 4-methyl-4′-methoxy benzophenone (4,4′-MMBP). The selectivity of the product (4,4′-MMBP) depends upon the type of the catalyst used in the reaction which may be attributed to the different reactivity

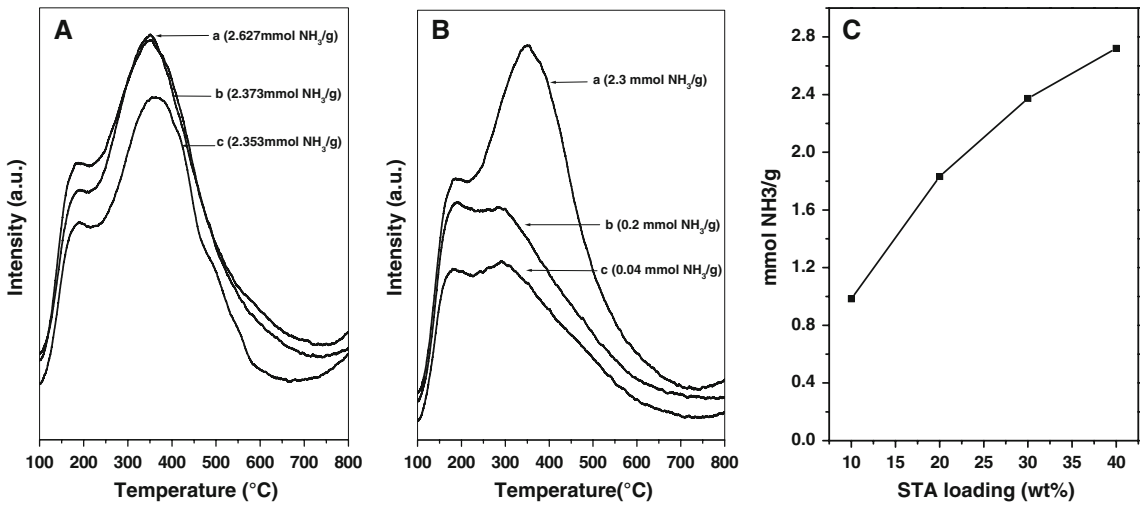

Fig. 6 Ammonina TPD profile for **A** (a) 30 wt% STA–ASW (b) 30 wt% STA–MA (c) 30 wt% STA–CB. **B** (a) 30 wt% STA–MA calcined at 250 °C (b) 30 wt% STA–MA calcined at 450 °C (c) 30 wt% STA–MA calcined at 650 °C and **C** Effect of STA loading on acidity

Table. 2 Catalytic activity of various catalysts

S. No.	Catalyst	Conversion (wt%)	Product distribution (wt%)		
			Ortho	Para	Meta
1	Blank	5.46	36.65	60.92	2.42
2	Pure STA[a]	73.24	6.24	87.89	5.92
3	$AlCl_3$	27.71	47.15	52.62	0.23
4	Al–MCM-41	6.50	80.42	18.69	0.97
5	W–meso-Al (W–MA)	39.10	19.68	76.29	4.03
6	Pure Support (MA)	13.92	94.69	5.09	0.22
7	30 wt% STA–ASW	72.68	21.69	74.54	3.60
8	30 wt% STA–MA	62.95	4.25	94.92	0.78
9	30 wt% STA–CB	56.22	9.74	85.91	4.36

Conditions: temperature = 120 °C, catalysts = 0.1 g, anisole/*p*-toluoyl chloride molar ratio = 1, time = 6h

[a] Amount of catalyst used = 30 mg

position of anisole over these catalysts. The conversion of anisole over Al–MCM-41, 30 wt% STA–ASW, 30 wt% STA–MA and 30 wt% ST–CB were found to be 6.50, 72.68, 62.95 and 56.22 wt%, respectively, whereas the corresponding para selectivity for 4,4′-MMBP were 18.69, 74.54, 94.92 and 85.91 wt%, respectively. Among the STA loaded catalysts, alumina synthesized without surfactant gave higher conversion compared to STA loaded MA and STA–CB, however the selectivity for 4,4′-MMBP was found to be higher over STA–MA than STA–ASW and STA–CB. The catalyst used in this study, shows the following decreasing order of activity after 6 h of reaction time: pure STA > 30-STA–ASW > 30-STA–MA > 30-STA–CB > W-MA > $AlCl_3$ > Pure Support > Al–MCM-41. Whereas the selectivity to para product is in the order of 30-STA–MA > pure MA support > pure STA > $AlCl_3$ > 30-STA–CB > Al–MCM-41 > W-MA > 30-STA–ASW. The high selectivity of 30-STA–MA may be due to uniform size of the mesopores than the other two alumina materials which is having wide range of pores which is clearly explained in the pore size distribution curve in the Fig. 2.

Acylation experiments were conducted using different STA loaded (5–40 wt%) catalysts and different calcination temperature of 30 wt%-STA–MA catalysts (Fig. 7). It is seen that the anisole conversion increased with increase in STA loading up to 30 wt% and then gets stabilized with further increase in loading. At the same time there is no appreciable change in para selectivity was observed with increase in STA loading. Further, to study the effect of calcination temperature, the catalyst was calcined at three different temperatures between 250 and 650 °C. The conversion of anisole decreases exactly half when the

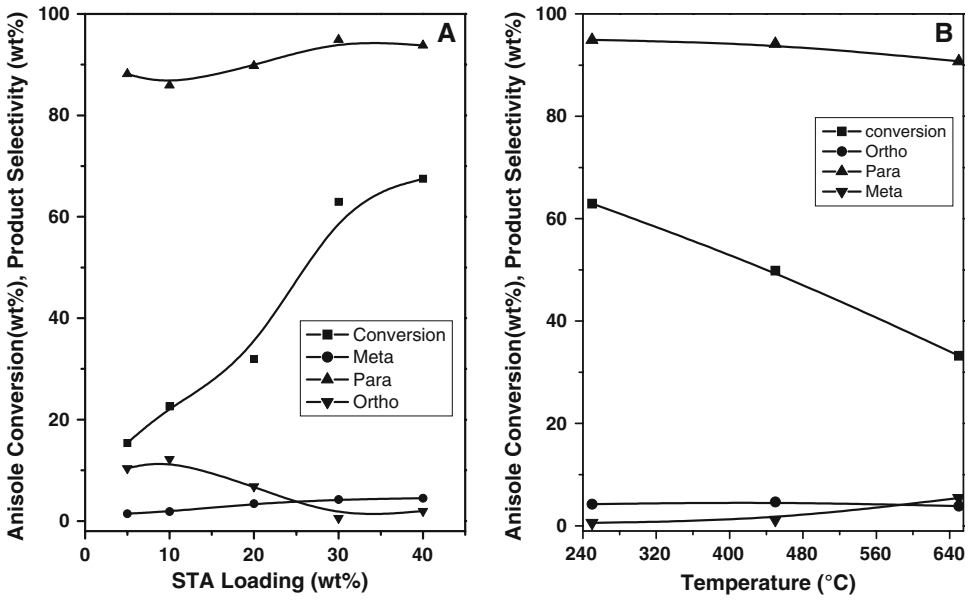

Fig. 7 Effect of **A** % loading of STA onto the MA and **B** calcination temperature of 30 wt% STA–MA on anisole conversion and product selectivity. Conditions: as mentioned in Table 2

calcination temperature increased from 250 to 650 °C. But there is no appreciable change in the product distribution. This may be due to the decomposition of keggin ion when the calcination temperature of the catalyst increased. This result is highly supported by the ammonia TPD profile (Fig. 6B), where the acidity of the catalyst decreases when the calcination temperature of the catalyst increased. This result clearly indicate that 30 wt% STA is needed for complete coverage of the mesoporous alumina support and the calcination temperature should be 250 °C for good conversion and selectivity.

3.8 Effect of Reaction Temperature

The acylation of anisole was carried out in the range 90–130 °C to know the effect of reaction temperature on the conversion of anisole and product selectivity by using 30 wt% STA loaded MA calcined at 250 °C. The results obtained are presented in Fig. 8. The conversion of anisole is increasing very slowly from 90° C to 110 °C. Once it reaches 120 °C the conversion is increased sharply, and it gets nearly level off after this temperature. There is no appreciable change in the para selectivity observed. One of the reasons for the increased rates at higher temperature may be ascribed to an enhancement of the rate of diffusion of anisole inside the channel of the catalyst, however, reaction rates are usually more temperature dependant than rate of diffusion.

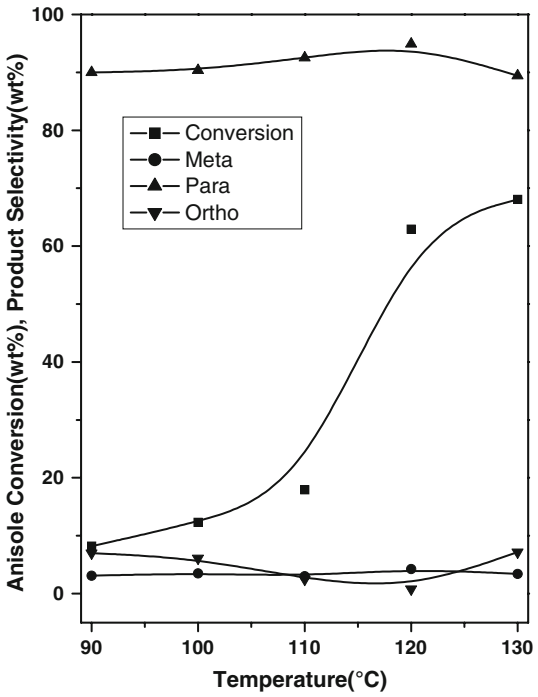

Fig. 8 Effect of reaction temperature on anisole conversion and product selectivity. Conditions: as mentioned in Table 2

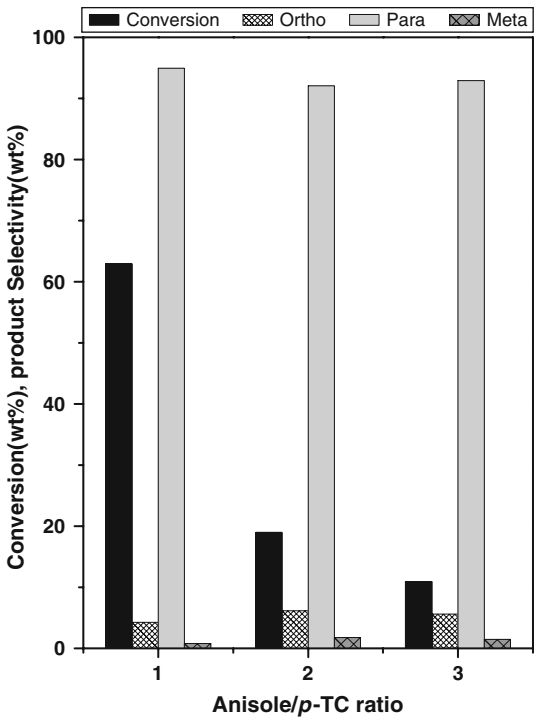

Fig. 9 Effect of anisole/*p*-TC ratio on anisole conversion and product selectivity. Conditions: as mentioned in Table 2

3.9 Influence of Molar Ratios of the Reactants

The results of the influence of anisole/*p*-toluoyl chloride molar ratios on the anisole conversion and product distribution is shown in Fig. 9. The ratios were changed by keeping the amount of *p*-TC as constant. The data show at 120 °C that, when anisole/*p*-TC ratio is increased from 1 to 3, the conversion of anisole decrease linearly from 62.9 to 10.9 wt%, respectively. From this result we can conclude that 1:1 molar ratio is good for high conversion of anisole and para selectivity for 4,4′-MMBP.

3.10 Influence of Catalyst/Anisole (w/w) Ratio

To study the effects of catalyst concentration on the conversion of anisole, rate of anisole conversion and product distribution, the catalyst (30% loaded) concentration (catalyst/anisole ratio (w/w)) was increased from 0.04 to 0.55 and the results are depicted in Fig. 10. The different ratios of catalyst/anisole were obtained by varying the amount of catalyst and keeping the concentration of anisole constant. The conversion of anisole increased from 25.4 to 62.9 wt% as the catalyst concentration increases from 0.04 to 0.18. The conversion gets nearly saturated when the ratio increased further. There is no much difference in the product distribution against the change in catalyst concentration.

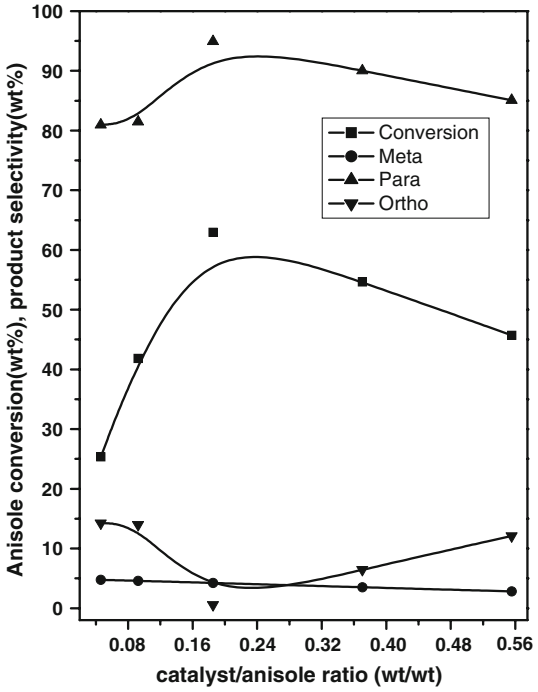

Fig. 10 Effect of catalyst/anisole ratio on anisole conversion and product selectivity. Conditions: as mentioned in Table 2

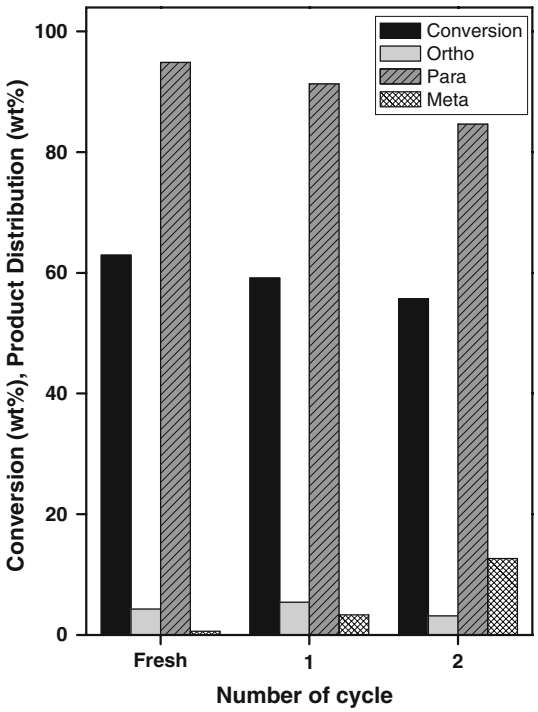

Fig. 11 Recycle experiment. Conditions: as mentioned in Table 2

3.11 Catalyst Recycling

Recycle of the synthesized catalysts was studied in the FC reaction of anisole with *p*-TC using 30 wt% STA–MA in order to check the stability and activity of recycled catalysts (Fig. 11). Three reaction cycles (fresh and two recycles) were carried out under similar reaction condition, using the same catalyst. After workup of the reaction mixture, the catalyst was separated by filtration, washed with acetone and activated for 10 h at 100 °C in the presence of air before use in the next experiment. The conversion of anisole over fresh, first and second recycling are found to be 62.9, 59.1, 55.7 wt%, respectively. The corresponding selectivity for 4,4′-MMBP are 94.9, 91.3, 84.6%, respectively. The little decrease in the conversion may be due to the partial leaching of the STA from the mesoporous alumina support.

4 Conclusion

In conclusion, MA has been synthesized by the lauric acid and aluminum sec-butoxide as the precursor. The calcined MA was functionalized with STA by wet impregnation method. Different loadings of STA over MA was carried out and characterized by various physico-chemical techniques to know the structural integrity and nature of support STA interaction. The activities of all the synthesized catalysts along with the conventional catalyst ($AlCl_3$) were checked in the FC acylation reaction of anisole with *p*-toluoyl chloride, which indicate that 30 wt% STA loaded on MA is showing good selectivity towards 4,4′-MMBP (94.92%) with moderate conversion of anisole (62.95 wt%). Among the different alumina support tested the anisole conversion is in the order ASW > MA > CB while the order of selectivity toward para product is MA > CB > ASW. The influence of the calcination temperature, catalyst concentration, reaction temperature and anisole/*p*-TC molar ratio on the catalyst performance is examined in order to optimize the conversion of anisole and selectivity to 4,4′-MMBP. The conversion of anisole using 30-STA–MA increased significantly with an increase in reaction time, catalyst concentration, and reaction temperature and decreased for anisole to *p*-TC molar ratio and calcination temperature. The para-selectivity of the catalyst is correlated with the pore size distribution and the catalyst, with uniform mesopores is giving more selectivity than the wide range of mesopores. No major loss of activity was observed after two recycles. The conversion of anisole and selectivity towards para product were 55.6 and 84.7 wt%, respectively at the end of the second cycle by using 30 wt% STA–MA as catalyst.

Acknowledgments SK thanks Council of Scientific and Industrial Research, New Delhi, for Senior Research Fellowship.

References

1. Xia YD, Hua WM, Tang Y, Goa Z (1999) Chem Commun 1899
2. Jin T, Yamaguchi T, Tanabe K (1986) J Phys Chem 90:4797
3. Hino M, Arata K (1979) J Chem Soc Chem Commun 1148
4. Corma A (1995) Chem Rev 95:559
5. Liu Z, Ji W, Dong L, Chen Y (1998) Mater Chem Phys 56:134
6. Kresge CT, Leonowicz ME, Roth WJ, Vartuli JC, Beck JS (1992) Nature 359:710
7. Beck JS, Vartuli JC, Roth WJ, Leonowicz ME, Kresge CT, Schmitt KD, Chu CTW, Olson DH, Sheppard EE, McCullen SB, Higgins JB, Schlenker JL (1992) J Am Chem Soc 114:10834
8. Antonelli DM, Ying JY (1996) Angew Chem Int Ed Engl 35:426
9. Antonelli DM, Ying JY (1996) Chem Mater 8:874
10. Terrible D, Trovarelli A, Llorca J, De Leitenburg C, Dolcettin G (1998) J Catal 178:299
11. Sayari A, Liu P (1997) Microporous Mater 12:149
12. Bagshaw SA, Pinnavaia TJ (1996) Angew Chem 108:1180
13. Bagshaw SA, Pinnavaia TJ (1996) Angew Chem Int Ed Engl 35:1102
14. Vaudry F, Khodabandeh S, Davis ME (1996) Chem Mater 8:1451
15. Cabrera S, Haskouri JE, Alamo J, Beltron A, Beltran D, Mendioroz S, Marcos MD, Amoros P (1999) Adv Mater 11:379
16. Kozhevnikov IV (1998) Chem Rev 98:171
17. Fournier M, Feumi-Jantou C, Rabia C, Herve G, Launay S (1992) J Mater Chem 2:971
18. Misono M (1987) Catal Rev Sci Eng 29:269
19. Misono M (1998) Catal Rev Sci Eng 30:339
20. Rocchiccioli-Deltcheff C, Amirouche M, Herve G, Founier M, Che M, Tatibouct JM (1990) J Mol Catal 126:591
21. Swanmi S, Shin-ichi N, Okuahar T, Misono M (1997) J Catal 166:263
22. Faming Z, Shenquing G, Shuoming S CN 1, 197, 057 (Cl, C07, C69/34) 28 October 1998, Applied; 97, 104, 061, 23 Apr 1997, 6 pp (Ch)
23. Vazquez PG, Blanco MN, Caceres V (1999) Catal Lett 60:205
24. Pizzio LR, Cacares CV, Blanco MN (1998) Appl Catal A 167:283
25. Schwegier MA, Vinke P, Vijk M, Bekkum H (1992) Appl Catal A 80:41
26. Izumi Y, Hasebe R, Urabe K (1983) J Catal 84:402
27. Dupont P, Vedrine JC, Paumard E, Hecquet G, Lefebve F (1995) Appl Catal A 129:217
28. Dupont P, Lefebve P (1996) J Mol Catal A 124:299
29. Kozhevnikov IV, Sinnema A, Jansen RJ, Panin K, Bekkum KV (1995) Catal Lett 30:241
30. Jalil PA, Al-Daous MA, Al-Arfaj ARA, Al-Amer AM, Beltramini J, Barri SAI (2001) Appl Catal A 207:159
31. Verhoef MJ, Kooyamann PJ, Peters JA, Bekkum HV (1999) Microporous Mesoporous Mater 27:365
32. Nomiya K, Murasaki H, Miwa M (1986) Polyhedron 5:1031
33. Devassy BM, Halligudi SB, Hegde SG, Halgeri AB, Lefebvre F (2002) Chem Commun 1074
34. Chen CY, Li HY, Davis ME (1993) Microporous Mater 2:17
35. Potdar HS, Jun KW, Bae JW, Kim SM, Lee YJ (2007) Appl Catal A Gen 321:109
36. Colomban PH (1988) J Mater Sci Lett 7:1324
37. Sawant DP, Vinu A, Jacob NE, Lefebvre F, Halligudi SB (2005) J Catal 235:341